Published in final edited form as:

Bone. 2015 July ; 76: 58–66. doi:10.1016/j.bone.2015.03.019.

In Vivo Mechanical Loading Rapidly Activates β–catenin Signaling in Osteocytes through a Prostaglandin Mediated Mechanism

N Lara-Castillo[1], **NA Kim-Weroha**[1], **MA Kamel**[1], **B Javaheri**[2], **DL Ellies**[3], **RE Krumlauf**[1,4], **G Thiagarajan**[5], and **ML Johnson**[1]

[1]UMKC School of Dentistry, Department of Oral and Craniofacial Sciences, Kansas City, MO 64108

[2]The Royal Veterinary College, Royal College Street, London, NW1 0TU, United Kingdom

[4]Stowers Institute for Medical Research, Kansas City, MO 64110

[5]UMKC School of Computing and Engineering, Kansas City, MO 64110

Abstract

The response of the skeleton to loading appears to be mediated through the activation of the Wnt/β-catenin signaling pathway and osteocytes have long been postulated to be the primary mechanosensory cells in bone. To examine the kinetics of the mechanoresponse of bone and cell types involved in the *in vivo*, we performed forearm loading of 17-week-old female TOPGAL mice. β-catenin signaling was observed only in embedded osteocytes, not osteoblasts, at 1 hour post loading, spreading to additional osteocytes and finally to cells on the bone surface by 24 hrs. This early activation at 1 hour appeared to be independent of receptor (Lrp5/6) mediated activation as it occurred in the presence of the inhibitors sclerostin and/or Dkk1. The COX-2 inhibitor, Carprofen, blocked the activation of β-catenin signaling and decline in sclerostin positive osteocytes post-loading implying an important role for prostaglandin. *In vitro*, PI3K/Akt activation was shown to be required for β-catenin nuclear translocation downstream from prostaglandin in MLO-Y4 osteocyte-like cells supporting this mechanism. Downstream targets of β-catenin signaling, sclerostin and Dkk1, were also examined and found to be significantly down regulated in osteocytes *in vivo* at 24 hours post-loading. The pattern of initially activated

Address Correspondence to: Mark L. Johnson, Ph.D., Professor and Chair, Department of Oral and Craniofacial Sciences, UMKC School of Dentistry, 650 East 25th Street, Kansas City, MO 64108, johnsonmark@umkc.edu.

[3]Current Address: OsteoGeneX Inc, Kansas City, KS 66103

NL-C performed data collection and analysis and preparation of the manuscript; NK-W performed data collection and analysis and portions of this manuscript were submitted as partial fulfillment of her Master's Degree in Oral Biology at UMKC; MAK and BJ performed data collection and analysis; DLE and REK assisted with the development of experimental methods and the initial design of experiments; GT performed the Finite Element Modeling and assisted with the writing of the manuscript.; MLJ is responsible for overall design and conduct of the experiments and preparation of the manuscript. All authors contributed to the final editing of the manuscript prior to submission.

osteocytes appeared random and in order to understand this heterogeneous expression, a novel finite element model of the strain field in the ulna was developed, which predicts highly variable local magnitudes of strain experienced by osteocytes. In summary, both *in vivo* and *in vitro* models show the rapid activation of β-catenin in response to load through the early release of prostaglandin and that strain fields in the bone are extremely heterogeneous resulting in heterogeneous activation of the β-catenin pathway in osteocytes *in vivo*.

Keywords

Osteocyte; mechanical loading; Wnt/β-catenin Signaling; prostaglandin

1. INTRODUCTION

The skeleton is known to adjust its mass and architecture to changes in load. However, the precise mechanism by which a physical signal such as applied mechanical load is converted into a biochemical signal(s) that alters various bone cell functions is not fully understood. Numerous studies have demonstrated that multiple bone cell types are capable of responding to mechanical loading[1], but it is the osteocyte that has been postulated to be the primary mechanosensory cell in bone[2–5]. The fact that the osteocyte is the most abundant cell in bone, is located within the mineralized matrix, and its interconnected lacunar-canalicular network make it ideally suited to be the primary mechanosensory cell in bone. Studies have shown primary chicken osteocytes and MLO-Y4 osteocyte-like cells[6] are much more sensitive to *in vitro* forms of loading versus osteoblastic cells[7–10], which further supports the role of the osteocyte as the primary mechanosensory cell.

Until recently, much of our cell/molecular understanding of mechanosensation in bone has largely been based upon cell culture models, but over the past decade new *in vivo* approaches have been developed to study the osteocyte within the bone environment[11,12]. *In vitro* studies have identified a number of important signaling molecules that are involved in the very rapid bone cell responses to mechanical loading such as NO[13,14], Ca^{+2} [15,16], ATP[15,17], and PGE_2 [17–19]. Conversely, *in vivo* studies have largely focused on late responses to mechanical loading such as new bone formation. However, some of these demonstrated increased metabolic activity in osteocytes and/or periosteal cells following short bouts of loading[20,21].

The discovery of mutations in the low density lipoprotein receptor related protein 5 (*LRP5*) gene as causal for human conditions of decreased and increased bone mass[22–24] demonstrated a role for the Lrp5/Wnt/β-catenin signaling pathway in bone mass regulation. This led to the hypothesis that the $LRP5^{G171V}$ or *HBM* mutation altered the sensitivity of the skeleton to mechanical loading[25]. It is now clearly established that loading activates the Wnt/β-catenin signaling pathway, *in vitro*[26–30] and *in vivo*[31–34]. Recently we have shown that the targeted deletion of a single allele of β–catenin in osteocytes abolishes the ability of the adult skeleton to form new bone in response to *in vivo* mechanical loading[35]. We and other groups have also shown both PGE_2 and PI3K/Akt signaling are involved in the activation of β–catenin signaling in response to loading in osteoblast, osteocyte and mesenchymal stem cell responses to loading[9,27,29,36].

All of these findings have established a critical role for the Wnt/β-catenin signaling pathway in the response of bone to mechanical loading. Given the widely held belief that the osteocyte is the mechanosensory cell in bone, we previously proposed a model that attempted to integrate PGE_2, PI3K/Akt and Wnt/β-catenin signaling to account for the response of the osteocyte to mechanical loading[3]. Here we provide *in vivo* evidence that activation of β–catenin signaling in response to loading occurs very rapidly, but in a subset of osteocytes that subsequently appear to propagate a load signal to surrounding osteocytes over time. We also provide *in vivo* and *in vitro* evidence that in the early stages of this response, activation of β–catenin signaling occurs independent of Lrp5 through crosstalk with other signaling pathways, notably prostaglandin and PI3K/Akt signaling. These findings confirm and extend our previous model of how osteocytes respond to mechanical load[3].

2. MATERIALS AND METHODS

2.1 Animals

The TOPGAL β-catenin reporter mouse which carries a *lacZ* gene under the control of the TCF/Lef promoter[37] was obtained from the Jackson Labs. 17-week old female TOPGAL mice were used for all studies. Originally on the CD-1 background, we have crossed this mouse with the C57Bl/6 (Jackson Labs) and the studies performed herein used littermates with the mixed genetic CD-1xC57BL/6 background. In one study, Carprofen (Pfizer, NY) was injected (5mg/Kg) 3 hours prior to loading. All protocols were approved by the UMKC Institutional Animal Care and Use Committee (IACUC).

2.2 Strain Gaging Analysis

Uniaxial strain gages (EA-06-015DJ-120-option, Vishay Micro-Measurements, Raleigh, NC, USA) were glued (Bond 200 kit, Vishay Micro-Measurements) to the ulna at the mid shaft on the medial surface. All forearm loading was performed using a Bose-Electroforce 3220 loading system (BOSE Corp., Minnetonka, MN, USA). Strain measurements were made using an electronic bridge conditioner Model 7000-32-SM (Vishay Micro Measurements) and analyzed using StrainSmart Software (Vishay Micro-Measurements). Conditions for the strain gaging were: loading at −0.5, −1.0, −1.5, −2.0, −2.5, −3.0 and −3.5N, at 2Hz, using a harversine waveform for 15 cycles. Strains in the last five cycles were average to determine the load:strain relationship.

2.3 *In Vivo* Forearm Loading

Based on the strain gage data, right forearm compression loading was performed at 2.25N, which represents a global strain of 2,250 microstrain (με) for 100 cycles at 2Hz. A single session of loading was chosen so that the initial response of β-catenin signaling could be observed at strain levels previously shown to be anabolic for new bone formation[32,35]. During the 50 second loading session, the animal was anesthetized with 3.5% isoflurane. Following loading the mice were returned to normal cage activity. Four mice were sacrificed at each of the time points of 1, 4, 24, 48 and 72 hours after the single loading session. The left forearm of each mouse served as the non-loaded control.

2.4 β-Galactosidase Staining

For all solutions deionized (Direct-Q UV System, Millipore Corp) water was used unless otherwise noted. Following euthanasia the loaded right and non-loaded left forearms were removed by cutting the humerus at mid-shaft and skin/muscle dissected away from the bones, care being taken to not remove the periosteal layer. We found that critical to the success of the whole bone β-Galactosidase staining was the fresh preparation of ice cold 4% paraformaldehyde (PFA) and specifically the use of PFA obtained from Alfa Aesar (Cat# 43368, 16% w/v aqueous solution, methanol free). The stock PFA solution was diluted with 10X PBS (Ambion, Cat# AM9625, pH 7.4) to give 4% PFA in 1X PBS final concentrations. $K_3Fe(CN)_6$, $K_4Fe(CN)_6{\cdot}3H_20$, deoxycholic acid (sodium salt) and N,N-Dimethylformamide (DMF) were purchased from Sigma (St. Louis, MO), 1M $MgCl_2$ and 1M Tris-HCl (pH 8.0) solutions were purchased from Ambion, NP-40 substitute was obtained from Fluka Chemical Company (Sigma, St. Louis, MO) and X-gal powder was obtained Invitrogen (Carlsbad, CA). 0.2M solutions of $K_3Fe(CN)_6$ and $K_4Fe(CN)_6{\cdot}3H_20$ (K3 and K4 solutions, respectively) were made fresh each time. The X-Gal buffer (1ml of 1 M $MgCl_2$, 100 μl of NP-40 substitute and 0.05 gm of deoxycholic acid and brought to 500 ml final volume with Direct-Q deionized water was pre-made and stored for several months at room temperature. The X-Gal powder was placed into solution at 40mg/ml in DMF and was made fresh each time. The Staining Buffer was made fresh each time and contained 19 ml of X-Gal buffer, 0.5 ml each of 0.2 M K3 and K4 solutions, 200 μl of Tris-HCl (pH 8.0) and 0.5 ml of X-Gal solution.

Prior to fixation, the skin/muscle removed forearms were cut at the wrist ulna/radius joint. The forearms were then fixed for a minimum of 60 minutes but no longer than 90 minutes on ice or at 4°C with gentle rocking, followed by 3 washes with 1X PBS for 5 min each. Individual forearms were placed in 15 ml tubes containing 12 ml of the Staining Buffer and placed in the dark for 36–40 hours at 32°C without shaking. The extent of staining was routinely checked at 24 hours and stopped when color development was adequate.

Following staining the forearms were washed three times in 1X PBS (5 minutes each wash) and then post-fixed in 4% PFA (as above) overnight at 4°C, then washed three times in 1X PBS and placed in Immunodecal (Decal Chemical Corp, Tallman, NY) for up to 3 days with changes into fresh Immunodecal each day. Routinely 15 ml of Immunodecal per bone was used. After decalcification, the bones were washed several times (minimum 5 times) in deionized water and then stored in 70% ethanol until paraffin processing and embedding (usually within 1–2 days). Paraffin embedding was performed with the following processing steps and times: graded ethanol (70%, 80%, 95% twice) for 1 hour each, 100% ethanol-glycerol (95 ml 100% ethanol + 5 ml glycerol) twice for 2 hours each, three times in Xylene for 1 hour each, twice in paraffin for 1 hour each followed by two more paraffin steps for 90 minutes each. Bones were then placed in paraffin blocks for sectioning. We analyzed a minimum of 15–20 ten micron thick sections taken over a 2 mm region that was ±1 mm of the midshaft of the ulna (~5–7 mm distal to the olecranon).

2.5 Immunohistochemistry

Sections in groups of three to five were placed on SuperFrost positive charged (Fisher Scientific) slides and dried for 3 hours at 58°C. Paraffin was removed by a sequential dips in xylene and rehydrated through graded washes of ethanol and water, and finally washed in 1X PBS. Sections were incubated in blocking solution (2.5% BSA, 1% donkey serum in PBS) overnight at 4 C. The following day, sections were incubated with primary antibody against: Sclerostin (R&D System Minneapolis, MN), Dkk1 (Abcam; Cambridge, MA), Dkk2 (R&D System; Minneapolis, MN), Dkk3 and Dkk4 (Santa Cruz Biotechnology; Santa Cruz, CA) at a 1:100 dilution for 4 hours at room temperature for sclerostin and overnight at 4 °C for Dkk1, 2, 3 and 4, followed by three washes for 5 minutes each wash. Then sections were incubated for 1 hour with Cy3 conjugated Donkey anti goat (or anti-rabbit) secondary antibody (Jackson ImmunoResearch Laboratories, West Grove, PA) (1:200 in blocking solution) and DAPI. Isotype matched non-immune IgG are used as a negative control for all immunostaining studies.

2.6 TOPGAL Mouse Bone Section Quantitation

Activation of β-catenin signaling was detected by β-galactosidase staining for reporter expression (blue colored cells). Bright field and fluorescent microscopy was performed using a Nikon Eclipse 800 microscope with a 20X objective. Images were imported into Photoshop and compiled to give a single full ulna cross-section. A template grid was then overlaid on the compiled image and cells in each grid were counted and scored as either positive or negative for β–galactosidase, sclerostin and/or Dkk1. Total osteocytes present were also counted from DAPI staining of the sections. Staining intensity of the cells was not quantitated, but a simple positive negative determination was made and the results of 2–3 independent “scorers” were averaged for each section.

2.7 Cell Culture

MLO-Y4 osteocyte-like cells were cultured as previously described[6]. Pulsatile fluid flow shear stress (FFSS) at 2 dynes/cm^2 for 2 hours was performed as previously described[9,36]. The Akt inhibitor (Akt-i) was purchased from US Biological (Marblehead, MA). Akt-i was added to the MLO-Y4 cells 15 minutes prior to starting and throughout the FFSS. Static controls had a media change at the same time as the shear stressed cells and the cells were placed in the incubator, and no FFSS was applied. We did not incubate MLO-Y4 in parallel chambers for our static controls due to the fact this cell line is very sensitive to movement and sliding cells in the parallel chambers will activate signaling mechanism that would interfere with our analysis. We perform FFSS in low serum containing media (0.1% fetal bovine serum- and 0.1% calf serum) as the presence of fresh serum in combination with the low shear stress of changing the media highly activates the PI3K/Akt pathway and potentially mask the results for this study. At the end of FFSS, four slides of cells were used for protein extraction using RIPA buffer containing a protease and phosphatase inhibitor cocktail (Sigma Aldrich, St Louis, MO, USA) and protein concentration determined using the BCA Protein Assay Kit (ThermoFisher Scientific; Rockford, IL). The remaining slides were fixed with 2%PFA/0.2% Triton X-100 and used for immunocytochemistry analysis.

2.8 Western Blotting

One microgram of protein was denatured in 5X SDS sample buffer, boiled for 10min and then loaded onto 10% Tris-HCl ready gels (Bio-Rad Laboratories, Hercules CA, USA). Protein was then transferred onto a nitrocellulose membrane (Bio-Rad Laboratories) by electrophoresis at 60v (constant) for 2 hours. The membrane was blocked with 5% nonfat dried milk in TBS that contained 0.1% tween-20 (TBS-T). Membrane was then incubated overnight with primary antibody against the phosphorylated form of Akt (S473) (Cell Signaling, Danvers, MA) diluted in 3%BSA/TBS-T at 4°C with constant shaking. Membrane was washed with TBS-T three times for 5min each and incubated with HRP-conjugated anti-rabbit secondary antibody for 1 hour at room temperature, followed by washing steps with TBS-T. Band intensity was developed using the SuperSignal® West Dura Extended Duration Substrate (Pierce Biotechnology Inc. Rockford, IL). The blots were then scanned using the Luminescent Image Analyzer LAS 4000 (FujiFilm Medical Systems USA, Inc., Stamford, CT, USA) and band intensity was determined using MultiGage software (FujiFilm Medical Systems USA).

2.9 Immunostaining to Detect β-catenin Nuclear Translocation

MLO-Y4 cells after FFSS or various treatments were rinsed twice in cold phosphate buffered saline (Ambion, Grand Island, NY), fixed in 2% paraformaldehyde (Alfa Aesar) containing 0.2% Triton X-100 for 10 minutes and then washed 3 times in PBS at room temperature for 10 minutes each. Slides were blocked with blocking solution [2.5% bovine serum albumin (BSA) 1% non-immune donkey serum in PBS] overnight at 4°C. Incubation with primary antibody against the active form of β–catenin (Millipore; Billerica, MA) at a concentration of 1:100 in blocking solution occurred at room temperature for 4 hours. Slides were washed three times with PBS and incubated for 1 hour with Cy-3 conjugated donkey anti-mouse antibody (1:200) (Jackson ImmunoResearch Labs) Alexa 488 phalloidin (Molecular Probes) at 1:250 dilution and DAPI at 1:250 dilution (Sigma) diluted in blocking solution. Isotype matched nonimmune antibodies are used as a negative control for all immunostaining studies. Coverslips were mounted onto glass slides using a 5% propylgallate 9:1 glycerol mounting media. After immunostaining, cells were photographed under 40X objective lens using a Nikon E800 microscope equipped with epifluorescence light.

2.10 Measurement of MLO-Y4 β–catenin Immunostaining Fluorescence Intensity

Measurement of the intensity of fluorescence was performed using a slight modification of a previously published method[38]. DAPI (excitation 405 nm, emission 400–450 nm), Cy-3 (excitation 550 nm, emission 570 nm) were captured to obtain separate images. Images were obtained as a 16-bit image and analyzed using ImageJ Software (NIH). To avoid variability of the data and being biased by the data, each field was selected by viewing nuclear staining (DAPI) to identify near-confluent healthy cells. At least five different regions of interest (ROI) were imaged to have an average of the staining.

For each ROI binary masks were created for the DAPI to define nuclear areas. Hybrid 2D Mean Filter plugin (3X3 pixel radius) was used to remove background and to approximate the distribution of staining to a median value. Automatic thresholding using the Isodata

algorithm for DAPI pictures was used to convert images to a binary mask. For the β-catenin images, background was subtracted using a rolling pen. Using the image calculator, the masks were subtracted from the β-catenin image to obtain the nuclear compartment. Quantitative fluorescence data was then exported from ImageJ generated histograms for each image into Microsoft Excel software.

2.11 Finite Element (FE) Analysis Modeling

The forearm macroFE model of the murine ulna and radius was developed first from microCT images with a 65 μm resolution in plane and 12 μm out of plane resolution. The microCT images were imported into MIMICS (www.materialise.com) where a tetrahedral FE mesh was constructed from over 1100 slices using a semi-automated thresholding procedure. The macroFE model was subjected to global 2 N loading in order to extract the displacement boundary conditions at the mid-point region of the ulna. Details of this model and its construction and validation have been presented previously[39,40]. To determine strain magnitudes at the osteocyte level we created a microFE model by selecting a region at the mid-point of the ulna consisting of 7 consecutive 12 μm thick serial histological sections and their corresponding microCT slices. The actual location of each osteocyte lacunae from the histologic section were incorporated into the microFE model and were represented by a single tetrahedral element with an approximate size of 10–12 micrometers in this first generation model. Bone in this microFE model was treated as an isotropic material (E=20 GPa) and the lacunae were treated as voids with a very low elastic modulus (E = 2 MPa). Displacement boundary conditions from the macroFE model were applied to the boundaries of the combined 7 section microFE model in order to determine the strain magnitudes at the osteocyte locations.

2.12 Statistical Analysis

β–galactosidase, sclerostin and/or Dkk1 positive cells were counted and expressed as a percentage of the total number of cells for both right loaded and left non-loaded control ulnae in the region of interest. The ratio of % positive cells in the right ulna to left ulna was calculated and expressed as the percent increase above or below 100%. ANOVA with Tukey post hoc tests to determine between groups differences or un-paired t-test as appropriate were performed with a $p<0.05$ used as the level of significance.

3. RESULTS

3.1 β-catenin signaling activation kinetics post-load

Based upon our strain gaging analysis we determined that in order to obtain the desired global strain of 2,250με we needed to apply 2.25N load in our loading regime. TOPGAL mice were used to investigate which bone cells activate β–catenin signaling in response to *in vivo* loading and to assess the kinetics of activation. Shown in Figure 1A are representative images from TOPGAL mice obtained at 1, 4 and 24 hours post load (right forearm) compared with the corresponding non-loaded control (left forearm). The percentage of β–galactosidase positive cells in the non-loaded left ulnas ranged between 10–15%, which reflects the baseline levels of β–catenin signaling in osteocytes during normal homeostasis. There was a statistically significant increase in the number of cells displaying activated β–

catenin signaling as early as 1 hour post load (Figure 1B). At 1 and 4 hours post-load the cells stained positive for β-galactosidase were osteocytes embedded within the central region of the cortical bone. The increase peaked at 24 hours and returned to baseline levels of positive cells by 72 hours post load (Figure 1B). At 24 hours post-load we observed β-galactosidase positive cells on the bone surfaces (Figure 1C).

3.2 Mechanism of early activation of β-catenin signaling

The pattern and rapid activation of β-catenin signaling, occurring first in a subpopulation of osteocytes in the mid-cortical regions of the ulna at the 1 hour time point, led us to investigate a potential mechanism(s) for this observation. It is known that mechanical loading applied to MLO-Y4 osteocyte-like cells results in the rapid release of PGE_2 into the media[9]. Also, anabolic responses of bone to loading are known to be prostaglandin and COX-2 dependent [41,42]. To test for a possible role of prostaglandin signaling crosstalk in this activation of β–catenin signaling, we pretreated mice for 3 hours prior to loading with the COX-2 inhibitor, Carprofen. Ulnae were then analyzed at 24 hours post-load for activation of β-catenin signaling and for changes in sclerostin. As shown in Figure 2A, Carprofen treatment completely blocked the activation of β–catenin signaling in osteocytes, supporting a role for prostaglandins in activation of the pathway. Interestingly, we also observed a consistently lower level of β-galactosidase staining in the non-loaded ulna in the Carprofen treated mice, consistent with the view that positive staining in non-loaded ulnae reflects the basal levels of β–catenin signaling in osteocytes during normal activity. Shown in Figure 2B, while loading decreased the number of sclerostin positive osteocytes in loaded ulnae, Carprofen prevented this decrease at 24 hours.

One major prostaglandin known to be released in bone by loading is $PGE_{2,}$ which binds the EP2 receptor in osteocytes [43]. Activation of EP2 leads to the downstream stimulation of the PI3K/Akt pathway, which is known to be involved the response to mechanical loading[44]. To further test the role of PGE_2 in β–catenin nuclear translocation, we pretreated the MLO-Y4 cells with Akt-i (1μM), an inhibitor that blocks phosphorylation (activation) of Akt and then subjected the cells to fluid flow shear stress. Western blot analysis demonstrated that the normally observed increase in phosphorylation of Akt after fluid flow shear stress is blocked in the presence of Akt-i (Figure 3A). Furthermore, nuclear translocation of β-catenin that occurs in response to fluid flow shear stress is also inhibited in the presence of Akt-i (Figure 3B).

3.3 Loading decreases osteocyte sclerostin and Dkk1

Previously Robling *et al.*,[33] demonstrated a significant decrease in sclerostin and Dkk1 gene expression at 24 hours post load. Figure 4A shows images from 24 hours post-loading from the same regions used for quantitating the number of β–galactosidase positive cells on the combined regions illustrated by the boxes in Figure 1A. Dkk2, Dkk3 and Dkk4 were not detectable by immunostaining in the sections from loaded or non-loaded bones (data not shown). Figure 4B shows the quantitation and kinetics of sclerostin and Dkk1 changes in the TOPGAL loaded and unloaded ulnae. The number of sclerostin or Dkk1 positive cells reached a significant decrease in at 24 hours and a returned to baseline by 48–72 hours. While it was not possible to directly quantitate the numbers of osteocytes positive for both

sclerostin and Dkk1 in a single section, analysis of adjacent serial sections indicates that both of these inhibitors are expressed in the same osteocyte.

This kinetic analysis of sclerostin and Dkk1 changes in osteocytes also provided further support for an Lrp5/6 independent activation mechanism as suggested by our Carprofen studies (Figure 2). We overlaid the bright field (TOPGAL staining) and fluorescent (sclerostin or Dkk1) photographic images from each section. Shown in Figure 5 is an example of the comparison from an ulna 1 hour post-load. We observed clear evidence of activation of the β-catenin signaling pathway in osteocytes regardless of whether they were positive or negative for sclerostin. The same was true for Dkk1 (not shown).

3.4 Micro-scale FE Model Predicts Heterogeneous Strain Distribution

Finally we investigated a potential mechanism for the heterogeneous activation pattern of β–catenin signaling in osteocytes observed at 1 hour post loading. This pattern is inconsistent with traditional Finite Element (FE) models in which strain fields are predicted to be uniform across subregions of bone [33,39,45–50]. This led us to investigate whether these macroscale FE models failed to reflect micro-heterogeneity in the strain fields [51,52], which would be more consistent with our TOPGAL mouse loading data. To investigate this we generated new FE models of the mouse forearm that incorporated the histologically determined locations of the osteocyte lacunae into our radius-ulna FE model of the forearm [39]. Simulations were performed to create a microscale FE model in which the lacunae elements were assigned an elastic modulus of 2 MPa while surrounding bone was assigned an elastic modulus of 20 GPa. The result of this analysis is shown in Figure 6, which illustrates strains at osteocyte lacuna from the middle slice of the 7 slice region used in the simulation. The simple inclusion of the osteocyte lacuna clearly converts the isobar type strain fields predicted from more traditional FE modeling commonly used in the bone field to a very heterogeneous strain distribution with high strain concentration observed around several osteocyte lacuna.

4. DISCUSSION

We have previously proposed a hypothetical model that describes the biochemical events occurring in osteocytes in response to mechanical load[3]. Activation of the β–catenin signaling pathway is known to be an important downstream event in response to mechanical loading, which initiates a number of changes in the expression of target genes[26,32,33] and that Lrp5[31] and β–catenin[35] are required for new bone formation. These prior studies raise several questions with respect to our understanding of how bone responds to mechanical loading. First, which cell is the first to respond to applied load, is it the osteocyte as has long been postulated? Second, how is Lrp5/Wnt/β-catenin the pathway activated in bone cells in response to load? Third, what is the time course (kinetics) of bone cell response relative to changes in Wnt pathway inhibitors (sclerostin and Dkk1)? Fourth, how does strain experienced by bone and bone cells relate to activation of the Lrp5/Wnt/β-catenin pathway?

Here, we demonstrate that *in vivo* activation of β–catenin signaling in response to a single short loading session specifically occurs first in osteocytes by 1 hour post load; reaches peak activation at 24 hours and returns to baseline by 72 hours (Figure 1). Interestingly, the

earliest responding cells are a subset of osteocytes residing in the mid-regions of cortical bone of the loaded ulnae rather than near the periosteal or endosteal surfaces bone surface. We observed no activation of β–catenin signaling in bone surface cells until 24 hours post load. One could argue that cells on the bone surface detect the load and relay a signal to the osteocytes, but this is not consistent with our observations. If load were perceived by cells on the bone surfaces it is difficult to envision a mechanism that would lead to the selective activation of a subset of osteocytes in the mid-region of the cortical bone, rather than a more general and widespread activation. The osteocyte lacunar-canalicular network has been shown to not only form gap junctions between osteocytes but also contact bone surface cells (reviewed in [3,5,53–56]). If a biochemical load signal were generated from the bone surface it seems logical that osteocytes closest to the surface would be the first to activate. This is not what we observed, rather our data show that osteocytes in the mid-cortical region are the first to be activated. In order for bone surface cells to trigger a response in these mid-cortical cells would require that osteocytes adjacent to the surface cells would be refractory to or bypassed by this signal, which is difficult to envision from a mechanistic standpoint. In light of the directionality of activation of β-catenin signaling from these more deeply embedded osteocytes to adjacent osteocytes and eventually cells on the bone surfaces, it is more logical to interpret these observations as indicating that it is the initially activated osteocytes that sense and relay the applied mechanical load. Further support for this conclusion comes from a recent study by Jing et al. [57], which demonstrated that osteocytes but not surface cells displayed unique Ca^{2+} oscillation in response to in situ mechanical loading.

Our observation of significantly increased β–catenin reporter activity at the 1 hour post-load time point suggests that a very rapid biochemical event is triggering this early activation, such as might occur with Ca^{2+} signaling and/or NO, ATP or PGE_2 production/release. Alternatively there could be an existing pool of a Wnt ligand that can be rapidly mobilized to bind Lrp5/6 and frizzled receptors to activate the pathway. We reasoned that if this very early activation were the result of loading induced gene expression (and protein synthesis) of a Wnt ligand, which then bound to the Lrp5/6-frizzled co-receptor complex, this might not be possible in 1 hour given that the TOPGAL reporter gene would then have to undergo transcriptional activation and subsequent protein synthesis of the β–galactosidase we detect in our method. We therefore considered an alternative mechanism involving crosstalk with another signaling pathway.

PGE_2 is a particularly attractive candidate for the primary inducer of this rapid response, as we have previously shown *in vitro* that it is capable of inducing β–catenin nuclear translocation in both osteoblastic and the MLO-Y4 osteocyte-like cell line[9]. In this study, we demonstrated *in vivo* roles for prostaglandin using Carprofen, which is a non-steroidal anti-inflammatory agent that blocks the production of prostaglandins such as PGE_2 by inhibiting COX-2 activity. Carprofen treatments prior to loading completely blocked the peak activation of β-catenin signaling in response to loading observed at 24 hours (Figure 2A). We chose to examine the 24 hour time point as this was when pathway activation occurred in the maximum number of osteocytes. A full understanding of the role of prostaglandins will require a series of additional kinetic studies to determine the effects of COX-2 inhibition on the early and later time points. However, given that sclerostin levels

did not decrease at 24 hours in the Carprofen treated loaded ulnae supports the notion that the 1 and 4 hour activation was absent as well as PGE_2 has been shown to inhibit the expression of the *Sost* gene[58,59], which is consistent with our observations. Further support for a role of PI3K/Akt signaling was obtained in our *in vitro* studies with the MLO-Y4 osteocyte-like cell line treated with Akt-i (an inhibitor of Akt phosphorylation) that was shown to inhibit both the fluid flow shear stress mediated increase in Akt phosphorylation and the subsequent nuclear translocation of β–catenin (Figure 3). Based on the Carprofen and Akt-i studies we propose that early activation of β–catenin signaling in osteocytes occurs through an Lrp5/6 and Wnt ligand independent mechanism involving stimulation by prostaglandins and subsequent activation of PI3K/Akt signaling [9,27–29,36,60], which crosstalks with the Wnt/β-catenin signaling pathway at the level of GSK-3β [27,29,61,62]. The observation that the activation of β–catenin signaling occurs in cells regardless of whether they express the Wnt signaling inhibitors, sclerostin and Dkk1 (Figure 5), also support our conclusion that the initial activation of the pathway might occur through an Lrp5/6 and Wnt ligand independent activation of the pathway. Collectively all of our data suggest that the rapid activation of β–catenin signaling in osteocytes is dependent upon stimulation of Akt signaling via prostaglandins.

Following the initial activation we observed an increase in the number of β–catenin signaling positive osteocytes reaching a maximum at 24 hours. One explanation for this observed kinetics is that the initially activated osteocytes produce a signal that is transmitted to adjacent osteocytes. The nature of this signal or pathway responsible for this propagation is unknown at this time. Alternatively it could be that the observed time course is a reflection of rapid versus slower responding osteocytes and it takes time for some osteocytes to accumulate sufficient β–galactosidase to be detected by our assays. Both of these explanations infer that there are differences in the nature or ability of some osteocyte populations to respond to a common signal. Interestingly, the pattern of osteocyte activation and decreases in sclerostin and Dkk1 we observed, which was predominantly in the medial and lateral regions of the ulna is spatially consistent with the regions of new bone formation that we and others have reported as a consequence of both short, multiple forearm loading sessions[33,35,63] and after a single bout of loading[64]. Furthermore, Moustafa et al.[47] demonstrated in a tibia loading model that the number of sclerostin positive osteocytes decreased at sites where increased osteogenesis was observed on the corresponding bone surface; but on surfaces where no new bone formation occurred there was no change in sclerostin in the underlying osteocytes. However, additional studies are needed to ascertain if this pattern of osteocyte Wnt/β-catenin pathway activation spatially and temporally directs where new bone formation occurs.

Previous studies have shown the importance of Lrp5 in the bone formation response to mechanical loading and changes in sclerostin/Dkk1 levels following loading [31,65]. Consistent with those studies we observed significant reductions in the number of sclerostin and Dkk1 positive osteocytes by 24 hours coinciding with the time when β–catenin activation in osteocytes reaches a peak (Figure 4). These results, taken together with the role of Lrp5 in new bone formation in response to load, suggest that later aspects of the spatial and temporal propagation of the activation in β-catenin signaling involves the Lrp5 co-

receptor. The reduction in sclerostin and Dkk1 would permit a transition in which activation of the signaling pathway could occur through Lrp5 involving induction of a Wnt ligand and paracrine signaling to adjacent cells. We are currently attempting to determine the role of Lrp5 in the propagation aspect of our model.

Another important finding from our studies relates to the strain distributions within bone that mechanical load generates and are thought to trigger bone cell responses[5]. Currently the standard types of finite element (FE) models predicting strain distributions within loaded bone depict uniform (isobar) type strain gradients[39,47]. However these models are inconsistent with the observed dispersed pattern of β-catenin activation in our TOPGAL mouse loading studies. These FE models of uniform strain fields do not explain how a subset of osteocytes activate β-catenin signaling at 1 hour post-load while many adjacent osteocytes that would be predicted to experience the same strains by these FE models do not activate at the same time. A plausible explanation is that the strain fields surrounding osteocytes and across bone are heterogeneous rather than uniform as suggested by the studies of Nicolella and colleagues[51,52]. We have built our first generation of FE models that incorporate osteocyte lacunae. The predicted strain fields in these lacuni included models (Figure 6) are much more heterogeneous, as previously demonstrated by Nicolella and colleagues[51,52]. The predictions of maximal strain regions from this lacuna model better match local strain with our biological data of the activation of β-catenin signaling at 1 hour post load (Figure 1A). This indicates that efforts to increase the level of sophistication of FE models and accurately predict *in vivo* processes need to incorporate the exact size, shape and orientation of the lacunae and other factors such as the heterogeneous material properties of bone. The ultimate goal is to build a model that is consistent with the observed biological behavior and will allow us to ascertain the strain threshold needed for osteocyte activation. Also of note is that we observed activation of β-catenin signaling in osteocytes along with changes in sclerostin and Dkk1 in regions undergoing compression or tension. This seems somewhat paradoxical in terms of how mechanical signals are integrated with bone and by the osteocytes. While we have no clear explanation for this observation, perhaps what is critical is the magnitude of change in strain, not necessarily the type of strain being applied that the osteocyte detects.

In conclusion, we have provided *in vivo* and *in vitro* evidence for the activation of β-catenin signaling in osteocytes as an early response to mechanical loading. Our data support a mechanism in which mechanical load initially activates β-catenin signaling in osteocytes via a prostaglandin and Akt mediated mechanism. Following this initial activation in subset of osteocytes activate there is a subsequent propagation of the “load signal” to adjacent osteocytes and eventually to cells on the bone surfaces. This propagation is connected to the decreased expression of the Lrp5/6 and Wnt ligand inhibitors, sclerostin and Dkk1, in the cells that subsequently activate β-catenin signaling. These data provide further support the role of the osteocyte as the primary mechanosensory cell in bone and the central role of the β-catenin signaling pathway in the response of bone to mechanical loading [3].

Acknowledgments

The authors thank Ms. Bonna Holladay, Mr. Mark Dallas and Dr. Shiva Kotha for their expert technical assistance, and Ms. Terri Johnson and Mr. J.P. Rey and the Histology Core at Stowers Medical Research Institute for their assistance in the development of the TOPGAL staining and processing methods of the mouse forearms. This work was supported by grants from the National Institutes of Health NIAMS R01 AR053949 and NIA P01 AG039355. The authors thank Dr. Lynda Bonewald for her critical review of this manuscript and Dr. Dan Nicolella for his helpful guidance with the FE modeling.

References

1. Rubin J, Rubin C, Jacobs CR. Molecular pathways mediating mechanical signaling in bone. Gene. 2006; 367(0):1–16. [PubMed: 16361069]
2. Aarden E, Burger E, Nijweide P. Function of osteocytes in bone. J Cell Biochem. 1994; 55(5):287–299. [PubMed: 7962159]
3. Bonewald LF, Johnson ML. Osteocytes, mechanosensing and Wnt signaling. Bone. 2008; 42:606–615. [PubMed: 18280232]
4. Klein-Nulend J, Bakker AD, Bacabac RG, Vatsa A, Weinbaum S. Mechanosensation and transduction in osteocytes. Bone. 2013; 54(2):182–190. [PubMed: 23085083]
5. Schaffler M, Cheung W-Y, Majeska R, Kennedy O. Osteocytes: Master Orchestrators of Bone. Calcified Tissue International. 2014; 94(1):5–24. [PubMed: 24042263]
6. Kato Y, Windle J, Koop B, Qiao M, Bonewald LF. Establishment of an Osteocyte-like Cell Line, MLO-Y4. J Bone Miner Res. 1997; 12:2014–2023. [PubMed: 9421234]
7. Klein-Nulend J, van der Plas A, Semeins CM, et al. Sensitivity of osteocytes to biomechanical stress in vitro. FASEB J. 1995; 9:441–5. [PubMed: 7896017]
8. Klein-Nulend J, Semeins CM, Ajubi NE, Nijweide PJ, Burger EH. Pulsating fluid flow increases nitric oxide (NO) synthesis by osteocytes but not periosteal fibroblasts--correlation with prostaglandin upregulation. Biochem Biophys Res Commun. 1995; 217(2):640–8. [PubMed: 7503746]
9. Kamel MA, Picconi JL, Lara-Castillo N, Johnson ML. Activation of beta-catenin signaling in MLO-Y4 osteocytic cells versus 2T3 osteoblastic cells by fluid flow shear stress and PGE(2): Implications for the study of mechanosensation in bone. Bone. 2010; 47(5):872–881. [PubMed: 20713195]
10. Reyes ML, Hernandez M, Holmgren LJ, Sanhueza E, Escobar RG. High-frequency, low-intensity vibrations increase bone mass and muscle strength in upper limbs, improving autonomy in disabled children. J Bone Miner Res. 2011; 26(8):1759–66. [PubMed: 21491486]
11. Webster DJ, Schneider P, Dallas SL, Müller R. Studying osteocytes within their environment. Bone. 2013; 54(2):285–295. [PubMed: 23318973]
12. Kalajzic I, Matthews BG, Torreggiani E, et al. In vitro and in vivo approaches to study osteocyte biology. Bone. 2013; 54(2):296–306. [PubMed: 23072918]
13. Johnson DL, McAllister TN, Frangos JA. Fluid flow stimulates rapid and continuous release of nitric oxide in osteoblasts. Am J Physiol. 1996; 271(E):E201–E208.
14. Klein-Nulend J, Helfrich MH, Sterck JGH, Semeins CM, Burger EH. Human Primary Bone Cells Respond to Fluid Flow with Rapid Production of Nitric Oxide by Endothelial Nitric Oxide Synthase. J Bone Miner Res. 1997; 112(S):S191.
15. Jorgensen NR, Geist ST, Civitelli R, Steinberg TH. ATP- and Gap Junction-dependent Intracellular Calcium Signaling in Osteoblastic Cells. J Cell Biol. 1997; 139:497–506. [PubMed: 9334351]
16. You J, Reilly GC, Zhen X, et al. Osteopontin Gene Regulation by Oscillatory Fluid Flow via Intracellular Calcium mobilization and Activation of Mitogen-activated Protein Kinase in MC3T3-E1 Osteoblasts. J Biol Chem. 2001; 276:13365–13371. [PubMed: 11278573]
17. Genetos DC, Geist DJ, Liu D, Donahue HJ, Duncan RL. Fluid Shear-Induced ATP Secretion Mediates Prostaglandin Release in MC3T3-E1 Osteoblasts. J Bone Min Res. 2005; 20:41–49.
18. Ajubi NE, Klein-Nulend J, Nijweide PJ, et al. Pulsating Fluid Flow Increases Prostaglandin Production by Cultured Chicken Osteocytes - A Cytoskeleton - Dependent Process. Biochem Biophy Res Comm. 1996; 225:62–68.

19. Ajubi NE, Lkein-Nulend J, Alblas MJ, Burger EH, Nijweide PJ. Signal transduction pathways involved in fluid flow-induced PGE2 production by cultured osteocytes. Am J Physiology. 1999; 276(E):E171–E178.
20. Donaldson CL, Hulley SB, Vogel JM, et al. Effect of prolonged bed rest on bone mineral. Metabolism. 1970; 19(12):1071–84. [PubMed: 4321644]
21. Skerry TM, Bitensky L, Chayen J, Lanyon LE. Early strain-related changes in enzyme activity in osteocytes following bone loading in vivo. J Bone Min Res. 1989; 4:783–788.
22. Gong Y, Slee RB, Fukai N, et al. LDL Receptor-Related Protein 5 (LRP5) Affects Bone Accrual and Eye Development. Cell. 2001; 107:513–523. [PubMed: 11719191]
23. Little RD, Carulli JP, Del Mastro RG, et al. A mutation in the LDL receptor-related protein 5 gene results in the autosomal dominant high-bone-mass trait. Am J Hum Genet. 2002; 70(1):11–9. [PubMed: 11741193]
24. Boyden LM, Mao J, Belsky J, et al. High Bone Density Due to a Mutation in LDL-Receptor-Related Protein 5. N Engl J Med. 2002; 346:1513–1521. [PubMed: 12015390]
25. Johnson ML, Picconi JL, Recker RR. The Gene for High Bone Mass. The Endocrinologist. 2002; 12:445–453.
26. Lau K-HW, Kapur S, Kesavan C, Baylink DJ. Up-Regulation of the Wnt, Estrogen Receptor, Insulin-like Growth Factor-I, and Bone Morphogenetic Protein Pathways in C57BL/6J Osteoblasts as Opposed to C3H/HeJ Osteoblasts in Part Contributes to the Differential Anabolic Response to Fluid Shear. J Biol Chem. 2006; 281:9576–9588. [PubMed: 16461770]
27. Sunters A, Armstrong VJ, Zaman G, et al. Mechano-transduction in Osteoblastic Cells Involves Strain-regulated Estrogen Receptor a-mediated Control of Insulin-like Growth Factor (IGF) I Receptor Sensitivity to Ambient IGF, Leading to Phosphatidylinositol 3-Kinase/AKT-dependent Wnt/LRP5 Receptor-independent Activation of beta-Catenin Signaling. Journal of Biological Chemistry. 2010; 285(12):8743–8758. [PubMed: 20042609]
28. Santos A, Bakker AD, Zandieh-Doulabi B, de Blieck-Hogervorst JM, Klein-Nulend J. Early activation of the beta-catenin pathway in osteocytes is mediated by nitric oxide, phosphatidyl inositol-3 kinase/Akt, and focal adhesion kinase. Biochem Biophys Res Commun. 2010; 391(1): 364–9. [PubMed: 19913504]
29. Case N, Thomas J, Sen B, et al. Mechanical Regulation of Glycogen Synthase Kinase 3β (GSK3β) in Mesenchymal Stem Cells Is Dependent on Akt Protein Serine 473 Phosphorylation via mTORC2 Protein. Journal of Biological Chemistry. 2011; 286(45):39450–39456. [PubMed: 21956113]
30. Case N, Ma M, Sen B, et al. Beta-catenin levels influence rapid mechanical responses in osteoblasts. J Biol Chem. 2008; 283(43):29196–205. [PubMed: 18723514]
31. Sawakami K, Robling AG, Ai M, et al. The Wnt Co-Receptor Lrp5 is Essential for Skeletal Mechanotransduction, but Not for the Anabolic Bone Response to Parathyroid Hormone Treatment. J Biol Chem. 2006; 281:23698–23711. [PubMed: 16790443]
32. Robinson JA, Chatterjee-Kishore M, Yaworsky P, et al. Wnt/b-Catenin Signaling is a Normal Physiological Response to Mechanical Loading in Bone. J Biol Chem. 2006; 281:31720–31728. [PubMed: 16908522]
33. Robling AG, Niziolek PJ, Baldridge LA, et al. Mechanical Stimulation of Bone In Vivo Reduces Osteocyte Expression of Sost/sclerostin. J Biol Chem. 2008; 283:5866–5875. [PubMed: 18089564]
34. Tu X, Rhee Y, Condon KW, et al. Sost downregulation and local Wnt signaling are required for the osteogenic response to mechanical loading. Bone. 2012; 50(1):209–217. [PubMed: 22075208]
35. Javaheri B, Stern A, Lara N, et al. Deletion of a single β-catenin allele in osteocytes abolishes the bone anabolic response to loading. Journal of Bone and Mineral Research. 2013:n/a–n/a.
36. Kitase Y, Barragan L, Jiang JX, Johnson ML, Bonewald LF. Mechanical induction of PGE(2) in osteocytes blocks glucocorticoid induced apoptosis through both the beta-catenin and PKA pathways. J Bone Miner Res. 2010; 25(12):2657–2668. [PubMed: 20578217]
37. DasGupta R, Fuchs E. Multiple Roles for Activated LEF/TCF Transcription Complexes during Hair Follicle Development and Differentiation. Development. 1999; 126:4557–4568. [PubMed: 10498690]

38. Noursadeghi M, Tsang J, Haustein T, et al. Quantitative imaging assay for NF-kappaB nuclear translocation in primary human macrophages. J Immunol Methods. 2008; 329(1–2):194–200. [PubMed: 18036607]
39. Lu Y, Thiagarajan G, Nicolella DP, Johnson ML. Load/strain distribution between ulna and radius in the mouse forearm compression loading model. Medical Engineering & Physics. 2012; 34(3): 350–356. [PubMed: 21903442]
40. Thiagarajan G, Lu Y, Dallas M, Johnson ML. Experimental and finite element analysis of dynamic loading of the mouse forearm. J Orthop Res. 2014; 32(12):1580–8. [PubMed: 25196694]
41. Li J, Burr DB, Turner CH. Suppression of Prostaglandin Synthesis with NS-398 Has Different Effects on Endocortical and Periosteal Bone Formation Induced by Mechanical Loading. Calcified Tissue International. 2002; 70(4):320–329. [PubMed: 12004337]
42. Kunnel JG, Igarashi K, Gilbert JL, Stern PH. Bone Anabolic Responses to Mechanical Load In Vitro Involve COX-2 and Constitutive NOS. Connective Tissue Research. 2004; 45(1):40–49. [PubMed: 15203939]
43. Cherian PP, Cheng B, Gu S, et al. Effects of Mechanical Strain on the Function of Gap Junctions in Osteocytes are Mediated through the Prostaglandin EP2 Receptor. J Biol Chem. 2003; 278:43146–43156. [PubMed: 12939279]
44. Armstrong VJ, Muzylak M, Sunters A, et al. Wnt/b-Catenin signaling is a Component of Osteoblastic Bone Cell Early Responses to Load-bearing and Requires Estrogen Receptor a. J Biol Chem. 2007; 282:20715–20727. [PubMed: 17491024]
45. Harris SE, Gluhak-Heinrich J, Harris MA, et al. DMP1 and MEPE expression are elevated in osteocytes after mechanical loading in vivo: Theoretical role in controlling mineral quality in the perilacunar matrix. J Mus Neuron Interact. 2007; 7(4):313–315.
46. Chennimalai Kumar N, Dantzig J, Jasiuk I, Robling A, Turner C. Numerical Modeling of Long Bone Adaptation due to Mechanical Loading: Correlation with Experiments. Annals of Biomedical Engineering. 2010; 38(3):594–604. [PubMed: 20013156]
47. Moustafa A, Sugiyama T, Prasad J, et al. Mechanical loading-related changes in osteocyte sclerostin expression in mice are more closely associated with the subsequent osteogenic response than the peak strains engendered. Osteoporosis International. 2012; 23(4):1225–1234. [PubMed: 21573880]
48. Willie BM, Birkhold AI, Razi H, et al. Diminished response to in vivo mechanical loading in trabecular and not cortical bone in adulthood of female C57Bl/6 mice coincides with a reduction in deformation to load. Bone. 2013; 55(2):335–346. [PubMed: 23643681]
49. Yang H, Butz KD, Duffy D, et al. Characterization of cancellous and cortical bone strain in the in vivo mouse tibial loading model using microCT-based finite element analysis. Bone. 2014; 66(0): 131–139. [PubMed: 24925445]
50. Patel TK, Brodt MD, Silva MJ. Experimental and finite element analysis of strains induced by axial tibial compression in young-adult and old female C57Bl/6 mice. Journal of Biomechanics. 2014; 47(2):451–457. [PubMed: 24268312]
51. Rath Bonivtch A, Bonewald LF, Nicolella DP. Tissue strain amplification at the osteocyte lacuna: A microstructural finite element analysis. J Biomech. 2006
52. Nicolella DP, Moravits DE, Gale AM, Bonewald LF, Lankford J. Osteocyte lacunae tissue strain in cortical bone. J Biomech. 2006; 39(9):1735–43. [PubMed: 15993413]
53. Bonewald LF. The amazing osteocyte. Journal of Bone and Mineral Research. 2011; 26(2):229–238. [PubMed: 21254230]
54. Komori T. Functions of the osteocyte network in the regulation of bone mass. Cell and Tissue Research. 2013; 352(2):191–198. [PubMed: 23329124]
55. Loiselle AE, Jiang JX, Donahue HJ. Gap junction and hemichannel functions in osteocytes. Bone. 2013; 54(2):205–212. [PubMed: 23069374]
56. Dallas SL, Prideaux M, Bonewald LF. The Osteocyte: An Endocrine Cell … and More. Endocrine Reviews. 2013; 34(5):658–690. [PubMed: 23612223]
57. Jing D, Baik AD, Lu XL, et al. In situ intracellular calcium oscillations in osteocytes in intact mouse long bones under dynamic mechanical loading. The FASEB Journal. 2014; 28(4):1582–1592.

58. Genetos DC, Yellowley CE, Loots GG. Prostaglandin E_2 Signals Through *PTGER2* to Regulate Sclerostin Expression. PLoS ONE. 2011; 6(3):e17772. [PubMed: 21436889]

59. Galea GL, Sunters A, Meakin LB, et al. Sost down-regulation by mechanical strain in human osteoblastic cells involves PGE2 signaling via EP4. Febs Letters. 2011; 585(15):2450–2454. [PubMed: 21723865]

60. Almeida M, Han L, Bellido T, Manolagas SC, Kousteni S. Wnt Proteins Prevent Apoptosis of Both Uncommitted Osteoblast Progenitors and Differentiated Osteoblasts by b-Catenin-dependent and -independent signaling Cascades Involving Src/ERK and Phophatidylinositol 3-Kinase/AKT. J Biol Chem. 2005; 280:41342–41351. [PubMed: 16251184]

61. Castellone MD, Teramoto H, Williams BO, Druey KM, Gutkind JS. Prostaglandin E_2 Promotes Colon Cancer Cell Growth Through a G_s-Axin-b-Catenin Signaling Axis. Science. 2005; 310:1504–1510. [PubMed: 16293724]

62. Marotti G, Cane V, Palazzini S, Palumbo C. Structure: Function Relationships in the Osteocyte. Ital J Min Electrolyte Metab. 1990; 35:707–715.

63. Mantila Roosa SM, Liu Y, Turner CH. Gene expression patterns in bone following mechanical loading. Journal of Bone and Mineral Research. 2011; 26(1):100–112. [PubMed: 20658561]

64. Sample SJ, Behan M, Smith L, et al. Functional Adaptation to Loading of a Single Bone Is Neuronally Regulated and Involves Multiple Bones. Journal of Bone and Mineral Research. 2008; 23(9):1372–1381. [PubMed: 18410233]

65. Saxon LK, Jackson BF, Sugiyama T, Lanyon LE, Price JS. Analysis of multiple bone responses to graded strains above functional levels, and to disuse, in mice in vivo show that the human Lrp5 G171V High Bone Mass mutation increases the osteogenic response to loading but that lack of Lrp5 activity reduces it. Bone. 2011; 49(2):184–193. [PubMed: 21419885]

HIGHLIGHTS

- The *in vivo* kinetics of activation of β-catenin signaling in bone following mechanical loading was determined.
- Activation of β-catenin signaling that occurs initially in a subset of osteocytes and peaks at 24 hours post-load.
- The early activation of β-catenin signaling following *in vivo* loading occurs through a prostaglandin mediated mechanism.
- Finite element models incorporating osteocyte lacunae better explain the observed pattern of initial osteocyte activation of β-catenin signaling.

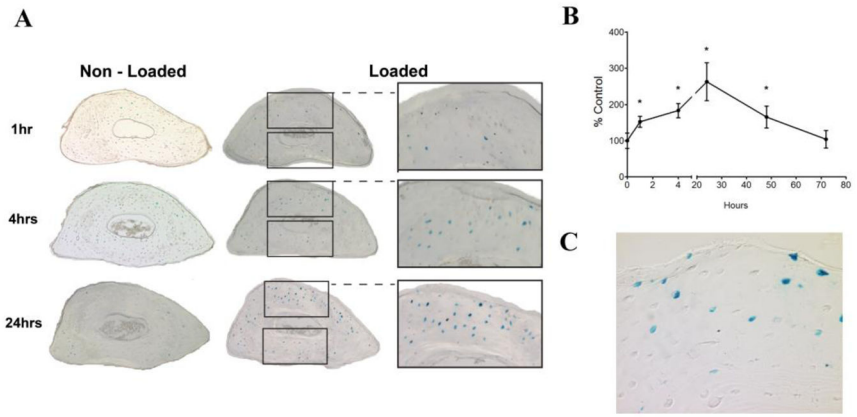

Figure 1.

Kinetics of β-catenin activation after a single load session. **A)** Representative images and close-up of cross-sections at the midshaft region of non-loaded and loaded ulnas **B)** Graph showing counts of manually counted β-catenin positive cells. Graph represents mean ± standard error of the mean (n=4, *p<0.05) **C)** Increased magnification view of a cross-section at the midshaft region of a loaded ulna (24 hour time point) illustrating activated cells at the bone surface.

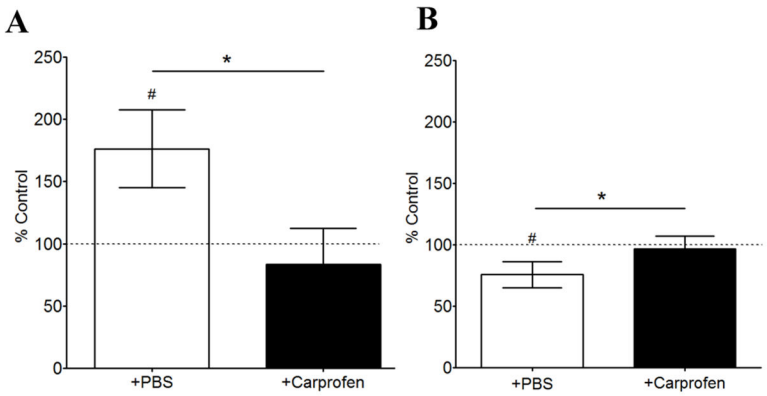

Figure 2.

Inhibition of COX-2 by Carprofen pre-treatment blocks the activation response of bone cells to loading. A) Graph of percentage of β-catenin positive cells in loaded versus non-loaded ulnae from mice treated with PBS or Carprofen. B) Graph of percentage of sclerostin positive cells in loaded versus non-loaded ulnae from mice treated with PBS or Carprofen. Carprofen was injected to animals 3 hours prior ulna compression. Data shown are from 24 hours post-load. Bars represent mean ± standard deviation (n=3 for PBS treated and n=4 for Carprofen treated group, *$p<0.05$ comparing Carprofen vs PBS control; #$p<.05$ loaded right ulnae vs non-loaded left ulnae).

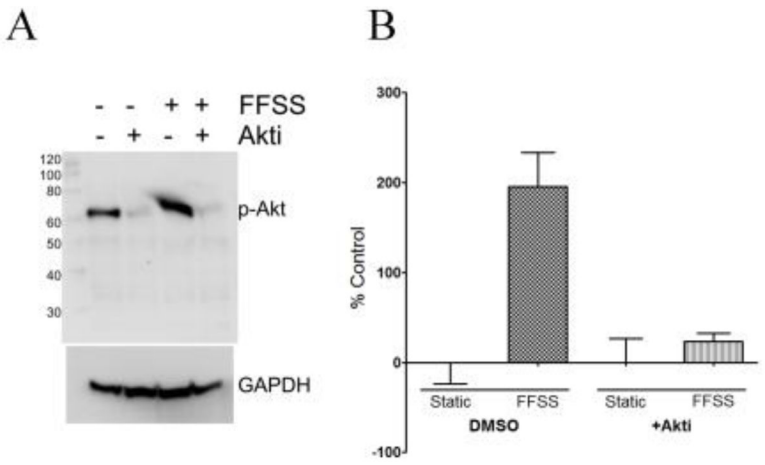

Figure 3.

Blocking Akt phosphorylation inhibits translocation of β-catenin to the nucleus **A)** Western blot showing inhibition of FFSS-induced Akt phosphorylation in the presence of Akt-i. **B)** Quantitation of β-catenin translocation to the nucleus (using ImageJ). Bars plot mean ± standard deviation. (n=4, *p<0.05)

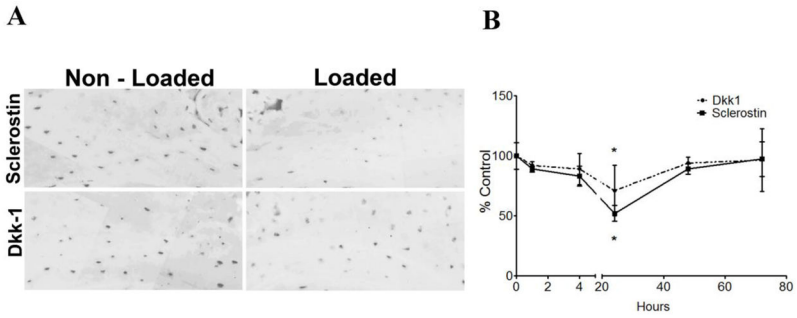

Figure 4.

Kinetics of sclerostin and Dkk1 expression after a single load session. **A)** Representative images showing expression of sclerostin and Dkk1 in ulna sections after 24 hours post load **B)** Graph showing counts of manually counted sclerostin and Dkk1 positive cells. Graph represents mean ± standard error of the mean (n=4, *p<0.05)

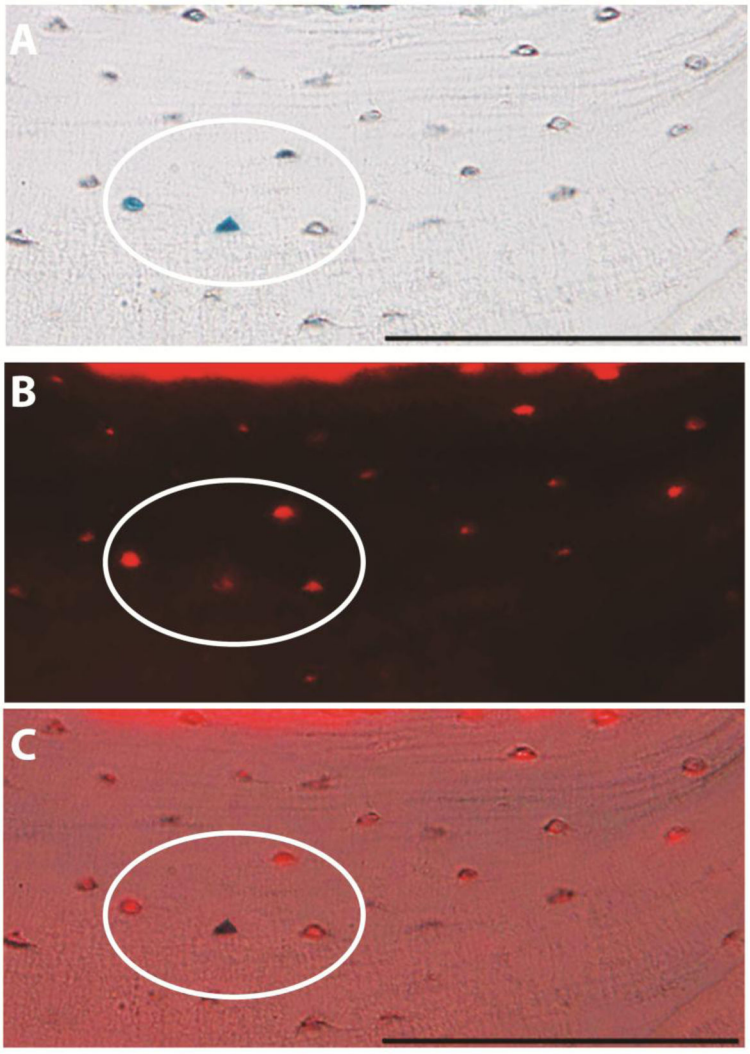

Figure 5.

Activation of β-catenin in the presence of the inhibitors of the Lrp5/Wnt/β-catenin pathway. **A)** Representative bright field image showing activation of β-catenin pathway (blue stained cells). **B)** shows the same section immunostained for sclerostin (red), and **C)** is the overlay of the top and middle images. Scale bar is 200μm.

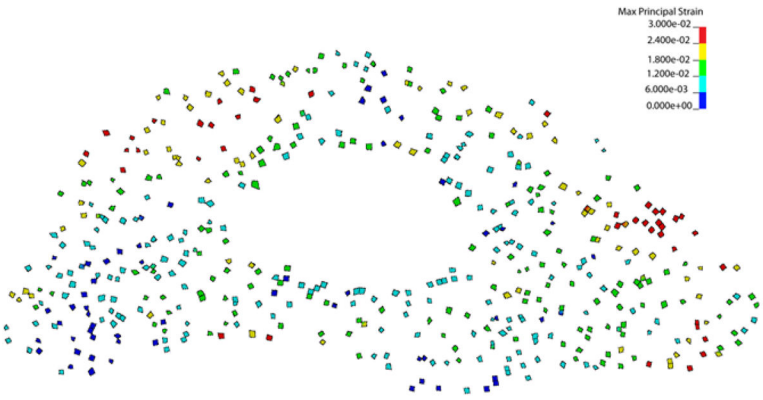

Figure 6.

Finite Element models of ulna midshaft. Osteocyte lacunae locations based upon corresponding histological sections were matched to microCT images of the bone modeled. Seven serial sections were included in the loading simulation and the FE predicted Max Principal Strains from the middle section is shown.